

PDRF: A general dispersion relation solver for magnetized multi-fluid plasma[☆]



Hua-sheng Xie^{*}

Institute for Fusion Theory and Simulation, Zhejiang University, Hangzhou, 310027, PR China

ARTICLE INFO

Article history:

Received 7 May 2013

Received in revised form

24 August 2013

Accepted 10 October 2013

Available online 25 October 2013

Keywords:

Plasma physics
Dispersion relation
Multi-fluid
Waves
Instabilities
Matrix eigenvalue

ABSTRACT

A general dispersion-relation solver that numerically evaluates the full propagation properties of all the waves in fluid plasmas is presented. The effects of anisotropic pressure, external magnetic fields and beams, relativistic dynamics, as well as local plasma inhomogeneity are included.

Program summary

Program title: PDRF

Catalogue identifier: AERF_v1_0

Program summary URL: http://cpc.cs.qub.ac.uk/summaries/AERF_v1_0.html

Program obtainable from: CPC Program Library, Queen's University, Belfast, N. Ireland

Licensing provisions: Standard CPC licence, <http://cpc.cs.qub.ac.uk/licence/licence.html>

No. of lines in distributed program, including test data, etc.: 436

No. of bytes in distributed program, including test data, etc.: 21,670

Distribution format: tar.gz

Programming language: MATLAB 7.

Computer: Any computer running MATLAB 7. Tested on DELL OptiPlex 380.

Operating system: Any system running MATLAB 7. Tested on Windows XP Pro.

RAM: 10 M

Classification: 10, 12, 15, 19.13.

Nature of problem:

This dispersion relation solver calculates all the solutions and gives corresponding polarizations for magnetized fluid plasma with arbitrary number of components and arbitrary orient wave vector, with and without anisotropic pressure, relativistic, beam and local inhomogeneity effects.

Solution method:

Solving as matrix eigenvalue problem.

Restrictions:

No kinetic and nonlinear effects.

Unusual features:

Giving all the solutions and polarizations.

Running time:

About 1 s on a Intel Pentium 2.60 GHz PC

© 2013 Elsevier B.V. All rights reserved.

[☆] This paper and its associated computer program are available via the Computer Physics Communication homepage on ScienceDirect (<http://www.sciencedirect.com/science/journal/00104655>).

^{*} Tel.: +86 13429672793; fax: +86 057 187953967.

E-mail addresses: huashengxie@gmail.com, huashengxie@126.com.

1. Introduction

Since only a few relatively simple dispersion relations in plasma physics are analytical tractable, it is of practical interest to develop general numerical schemes for obtaining and solving the dispersion relations of given plasma systems. Traditionally, one

obtains the dispersion relations from the determinant of the corresponding dielectric tensor for the eigenvalues of the wave solutions, such as that of the kinetic code WHAMP (Waves in Homogeneous Anisotropic Multicomponent Magnetized Plasma) by Ronnmark [1,2] and the *Mathematica* fluid code for magnetized parallel beam plasmas by Bret [3]. It is however difficult to generalize such treatments to include the arbitrary number of fluid species with good convergence or to obtain all the solutions of a given system.

In this work, we use a full-matrix approach to transform the task of obtaining the dispersion relations to an equivalent matrix eigenvalue problem by introducing a general dispersion relation solver PDRF (Plasma Dispersion Relation–Fluid Version) for magnetized multi-fluid plasmas including anisotropic, relativistic, beam and weak inhomogeneity effects. Our solver should be useful for investigating wave propagation properties in astrophysical, space, laser, and laboratory plasmas.

2. Theory and method

We consider a multi-fluid plasma in an external magnetic field $\mathbf{B}_0 = (0, 0, B_0)$. The flow velocity of the fluid component j is $\mathbf{v}_{j0} = (v_{j0x}, v_{j0y}, v_{j0z})$. The species densities are allowed to be locally inhomogeneous, with $\nabla n_{j0}/n_{j0} = (\epsilon_{njx}, \epsilon_{njy}, 0) = \text{constant}$. For simplicity, temperature gradient effects are ignored, and the wave vector is assumed to be $\mathbf{k} = (k_x, 0, k_z) = (k \sin \theta, 0, k \cos \theta)$. We do not need to obtain the 3 by 3 dispersion relation matrix for $\mathbf{E} = (E_x, E_y, E_z)$, as done in many existing analytical or numerical treatments, such as in Stix [4], Ronnmark [1,2] and Bret [3]. Instead, we use the original full dispersion relation matrix and treat it as a matrix eigenvalue problem, instead of directly solving for its determinant.

2.1. Governing equations

We start with the fluid equations

$$\partial_t n_j = -\nabla \cdot (n_j \mathbf{v}_j), \quad (1a)$$

$$\partial_t \mathbf{u}_j = -\mathbf{v}_j \cdot \nabla \mathbf{u}_j + \frac{q_j}{m_j} (\mathbf{E} + \mathbf{v}_j \times \mathbf{B}) - \frac{\nabla P_j}{\rho_j} - \sum_i (\mathbf{u}_i - \mathbf{u}_j) v_{ij}, \quad (1b)$$

$$\partial_t \mathbf{E} = c^2 \nabla \times \mathbf{B} - \mathbf{J}/\epsilon_0, \quad (1c)$$

$$\partial_t \mathbf{B} = -\nabla \times \mathbf{E}, \quad (1d)$$

where $\mathbf{u}_j = \gamma_j \mathbf{v}_j$, and

$$\mathbf{J} = \sum_j q_j n_j \mathbf{v}_j, \quad (2a)$$

$$d_t (P_{\parallel j} \rho_j^{-\gamma_{\parallel j}}) = 0, \quad (2b)$$

$$d_t (P_{\perp j} \rho_j^{-\gamma_{\perp j}}) = 0, \quad (2c)$$

where $\rho_j \equiv m_j n_j$, $c^2 = 1/\mu_0 \epsilon_0$, $\gamma_j = (1 - v_j^2/c^2)^{-1/2}$, and $\gamma_{\parallel j}$ and $\gamma_{\perp j}$ are the parallel and perpendicular adiabatic coefficients, respectively. Furthermore, $P_{\parallel, \perp} = n T_{\parallel, \perp}$, $\mathbf{P} = P_{\parallel} \hat{\mathbf{b}} \hat{\mathbf{b}} + P_{\perp} (\mathbf{I} - \hat{\mathbf{b}} \hat{\mathbf{b}})$ and $\hat{\mathbf{b}} = \mathbf{B}/B$. Note that our anisotropy model differs from that of CGL [6], but can be reduced to that of Bret and Deutsch [5] by setting $\gamma_{\parallel j} = \gamma_{\perp j} = \gamma_j$. By further setting $T_{\perp j} = T_{\parallel j}$, we can recover the isotropic pressure case.

After linearizing, (2) becomes

$$\mathbf{J} = \sum_j q_j (n_{j0} \mathbf{v}_{j1} + n_{j1} \mathbf{v}_{j0}), \quad (3a)$$

$$P_{\parallel, \perp j1} \equiv c_{\parallel, \perp j}^2 n_{j1}, \quad (3b)$$

where $c_{\parallel, \perp j}^2 = \gamma_{\parallel, \perp j} P_{\parallel, \perp j0} / \rho_{j0}$ and $\mathbf{P}_{j0} = n_{j0} \mathbf{T}_{j0}$. We note that

$$\nabla \cdot \mathbf{P}_{j1} = (ik_x, 0, ik_z) \cdot \begin{bmatrix} P_{\perp j1} & 0 & \Delta_j B_{x1} \\ 0 & P_{\perp j1} & \Delta_j B_{y1} \\ \Delta_j B_{x1} & \Delta_j B_{y1} & P_{\parallel j1} \end{bmatrix}, \quad (4)$$

where $\Delta_j \equiv (P_{\parallel j0} - P_{\perp j0})/B_0$ and $\beta_{\parallel, \perp j} = 2\mu_0 P_{\parallel, \perp j}/B_0^2$. The off-diagonal terms coming from the tensor rotation (see similar expressions in Appendix A) from $\hat{\mathbf{b}}_0$ to $\hat{\mathbf{b}}$ are related to energy exchange and are important for the anisotropic instabilities. An incorrect treatment or ignoring these off-diagonal terms can cause loss of the firehose and other unstable anisotropic modes.

2.2. Full-matrix treatment

The linearized version of (1) with $f = f_0 + f_1 e^{i\mathbf{k} \cdot \mathbf{r} - i\omega t}$, $f_1 \ll f_0$ is equivalent to a matrix eigenvalue problem

$$\lambda \mathbf{A} \mathbf{X} = \mathbf{M} \mathbf{X}, \quad (5)$$

with $\lambda = -i\omega$ the eigenvalue and \mathbf{X} the corresponding eigenvector, which also gives the polarization of each normal/eigenmode solution. Similar treatments can be found in [7] for the MHD equations and [8] for the ten-moment equations.

Accordingly, we have $\mathbf{X} = (n_{j1}, v_{j1x}, v_{j1y}, v_{j1z}, E_{1x}, E_{1y}, E_{1z}, B_{1x}, B_{1y}, B_{1z})^T$, $\mathbf{u}_{j1} = \gamma_{j0} [\mathbf{v}_{j1} + \gamma_{j0}^2 (\mathbf{v}_{j0} \cdot \mathbf{v}_{j1}) \mathbf{v}_{j0}/c^2] = \{a_{j pq}\} \cdot \mathbf{v}_{j1}$ ($p, q = x, y, z$), $\gamma_{j0} = (1 - v_{j0}^2/c^2)^{-1/2}$, and \mathbf{A} is given by

$$\begin{bmatrix} 1 & 0 & 0 & 0 & 0 & 0 & 0 & 0 & 0 & 0 \\ 0 & a_{jxx} & a_{jxy} & a_{jxz} & 0 & 0 & 0 & 0 & 0 & 0 \\ 0 & a_{jyx} & a_{jyy} & a_{jyz} & 0 & 0 & 0 & 0 & 0 & 0 \\ 0 & a_{jzx} & a_{jzy} & a_{jzz} & 0 & 0 & 0 & 0 & 0 & 0 \\ 0 & 0 & 0 & 0 & 1 & 0 & 0 & 0 & 0 & 0 \\ 0 & 0 & 0 & 0 & 0 & 1 & 0 & 0 & 0 & 0 \\ 0 & 0 & 0 & 0 & 0 & 0 & 1 & 0 & 0 & 0 \\ 0 & 0 & 0 & 0 & 0 & 0 & 0 & 1 & 0 & 0 \\ 0 & 0 & 0 & 0 & 0 & 0 & 0 & 0 & 1 & 0 \\ 0 & 0 & 0 & 0 & 0 & 0 & 0 & 0 & 0 & 1 \end{bmatrix}. \quad (6)$$

For simplicity, the relativistic effects in the friction terms v_{ij} are ignored. The matrix \mathbf{M} is then given by (v_{ij} terms when $i \neq j$ are not given explicitly here) Eq. (7) (see Box 1).

Furthermore,

$$\{a_{j pq}\} \equiv \begin{bmatrix} a_{jxx} & a_{jxy} & a_{jxz} \\ a_{jyx} & a_{jyy} & a_{jyz} \\ a_{jzx} & a_{jzy} & a_{jzz} \end{bmatrix} = \begin{bmatrix} \gamma_{j0} + \gamma_{j0}^3 v_{j0x}^2/c^2 & \gamma_{j0}^3 v_{j0x} v_{j0y}/c^2 & \gamma_{j0}^3 v_{j0x} v_{j0z}/c^2 \\ \gamma_{j0}^3 v_{j0x} v_{j0y}/c^2 & \gamma_{j0} + \gamma_{j0}^3 v_{j0y}^2/c^2 & \gamma_{j0}^3 v_{j0y} v_{j0z}/c^2 \\ \gamma_{j0}^3 v_{j0x} v_{j0z}/c^2 & \gamma_{j0}^3 v_{j0z} v_{j0y}/c^2 & \gamma_{j0} + \gamma_{j0}^3 v_{j0z}^2/c^2 \end{bmatrix}. \quad (8)$$

For a plasma containing s species of particles, the dimensions of \mathbf{A} and \mathbf{M} are $(4s + 6) \times (4s + 6)$. We can get all the linear harmonic wave solutions of the system without any convergence difficulty using a standard matrix eigenvalue solver, e.g., LAPACK or the function *eig()* in *MATLAB*. Here, a *MATLAB* code PDRF for solving the above eigenvalue problem is provided. By setting γ_j to 1, i.e., $\mathbf{A} = \mathbf{I}$ and $\{a_{j pq}\} = \mathbf{I}$, PDRF reduces to the non-relativistic case.

2.3. Validity

For the perturbation analysis, we have assumed $Q_0 = \sum_j q_j n_{j0} \sim 0$, $\mathbf{J}_0 = \sum_j q_j n_{j0} \mathbf{v}_{j0} \sim 0$, $\mathbf{v}_{j0} \cdot \nabla n_{j0} \sim 0$ and $\mathbf{F}_{j0} = q_j \mathbf{E}_0 + q_j (\mathbf{v}_{j0} \times \mathbf{B}_0) - \nabla P_{j0}/n_{j0} - m_j \sum_i (\mathbf{v}_{i0} - \mathbf{v}_{j0}) v_{ij} \sim 0$. In practice, these

n_{j1} should be $m_{j1} n_{j1}$

$$\begin{bmatrix}
 -i\mathbf{k} \cdot \mathbf{v}_{j0} & -ik_x n_{j0} - \epsilon_{nij} n_{j0} & -\epsilon_{nij} n_{j0} & -ik_z n_{j0} & 0 & 0 & 0 & 0 & 0 & 0 \\
 \frac{-ik_x c_{\perp j}^2}{\rho_{j0}} & b_{jxx} & b_{jxy} + \omega_{cj} & b_{jxz} & \frac{q_j}{m_j} & 0 & 0 & -\frac{ik_z \Delta_j}{m_j n_{j0}} & \frac{q_j v_{j0z}}{m_j} & \frac{q_j v_{j0y}}{m_j} \\
 0 & b_{jyx} - \omega_{cj} & b_{jyy} & b_{jyz} & 0 & \frac{q_j}{m_j} & 0 & \frac{q_j v_{j0z}}{m_j} & -\frac{ik_z \Delta_j}{m_j n_{j0}} & -\frac{q_j v_{j0x}}{m_j} \\
 \frac{-ik_z c_{\perp j}^2}{\rho_{j0}} & b_{jzx} & b_{jzy} & b_{jzz} & 0 & 0 & \frac{q_j}{m_j} & -\frac{q_j v_{j0y}}{m_j} - \frac{ik_x \Delta_j}{m_j n_{j0}} & \frac{q_j v_{j0x}}{m_j} & 0 \\
 -\frac{q_j v_{j0x}}{q_j n_{j0}} & -\frac{q_j n_{j0}}{q_j n_{j0}} & 0 & 0 & 0 & 0 & 0 & 0 & -ik_z c^2 & 0 \\
 -\frac{\epsilon_0}{q_j v_{j0y}} & \epsilon_0 & -\frac{q_j n_{j0}}{\epsilon_0} & 0 & 0 & 0 & 0 & ik_z c^2 & 0 & -ik_x c^2 \\
 -\frac{\epsilon_0}{q_j v_{j0z}} & 0 & 0 & -\frac{q_j n_{j0}}{\epsilon_0} & 0 & 0 & 0 & 0 & ik_x c^2 & 0 \\
 \epsilon_0 & 0 & 0 & \epsilon_0 & 0 & ik_z & 0 & 0 & 0 & 0 \\
 0 & 0 & 0 & 0 & 0 & -ik_z & 0 & ik_x & 0 & 0 \\
 0 & 0 & 0 & 0 & -ik_z & 0 & ik_x & 0 & 0 & 0 \\
 0 & 0 & 0 & 0 & 0 & -ik_x & 0 & 0 & 0 & 0
 \end{bmatrix}, \quad (7)$$

where $\omega_{cj} = q_j B_0 / m_j$, $q_e = -e$, $\omega_{pj}^2 = n_{j0} q_j^2 / \epsilon_0 m_j$, and $\{b_{j pq}\} = v_{jj} - i(\mathbf{k} \cdot \mathbf{v}_{j0}) \cdot \{a_{j pq}\}$.

Box I.

Table 1
Validity of the linearization.

-	1	2	3	4	5	6	7
Case $\neq 0$	$\sum_j q_j n_{j0}$	$\sum_j q_j n_{j0} \mathbf{v}_{j0}$	\mathbf{E}_0	$\nabla \mathbf{P}_{j0}$	$\mathbf{v}_{j0} \times \mathbf{B}_0$	$\sum_i (\mathbf{v}_{i0} - \mathbf{v}_{j0}) v_{ij}$	$\mathbf{v}_{j0} \cdot \nabla n_{j0}$

Table 2
Comparison of the cold plasma solutions using the matrix method and Swanson's polynomial method [9].

ω^M	± 10.5152	± 10.0031	± 9.5158	$\pm (2.4020\text{E}-4 - i8\text{E}-19)$	$\pm (1.1330\text{E}-4 - i1\text{E}-16)$	± 0	± 0
ω^S	± 10.5152	± 10.0031	± 9.5158	$\pm 2.4020\text{E}-4$	$\pm 1.1330\text{E}-4$	-	-

often-used assumptions may not always be valid. For example, a finite external current \mathbf{J}_0 would be associated with an external \mathbf{B}_{0j} field. To determine the latter, we will need the boundary conditions or other information. That could also mean that the system is no longer homogeneous. For example, a local current can generate an inhomogeneous magnetic field around it. Such finite lowest-order quantities cannot be removed by simple coordinate transformations. Similar difficulties can appear for non-parallel external beams. On the other hand, finite $\mathbf{v}_{\perp 0}$ is allowed if there are external electric fields, local inhomogeneities, gravitational force, etc., in the perpendicular direction. Moreover, when global gradient or inhomogeneity effects are included, the system will not be near uniform and a full treatment including the space dependent lowest order terms as well as the appropriate boundary conditions are required. However, here we are interested only in the local perturbations, so that the harmonic analysis, namely an $e^{i\mathbf{k} \cdot \mathbf{r} - i\omega t}$ dependence for the first order (linear) quantities, can still be used [4]. Possible breakdowns of the assumptions in PDRF are summarized in Table 1.

3. Benchmarks

3.1. Cold plasma

The numerical solutions ω^M of (5) and that ω^S of Swanson's fifth order polynomial method [9] for a cold two-component plasma in the absence of an external beam are shown in Table 2, for $kc = 0.1$, $\theta = \pi/3$, $m_i/m_e = 1836$ and $\omega_{pe} = 10\omega_{ce}$ (note: hereafter, $\omega_{cj} = |\omega_{cj}|$). We see that the two results are fully consistent. The small difference ($< 10^{-15}$) can be attributed to numerical errors. The dispersion curves for $\omega_{r,i}$ versus k and θ are given in Fig. 1, for $m_i/m_e = 4$ and $\omega_{pe} = 2\omega_{ce}$.

3.2. The firehose and mirror instabilities

Two well-known low-frequency hydromagnetic anisotropic instabilities are the firehose and mirror instabilities. The dispersion relation for the firehose (or, anisotropic shear Alfvén) mode is $(\frac{\omega}{k_z v_A})^2 \simeq 1 + \sum_j \frac{\beta_{\perp j} - \beta_{\parallel j}}{2}$. For $k_z \ll k_{\perp}$, using the reduced expression from the bi-Maxwellian dispersion relation, we can obtain the mirror instability threshold $1 + \sum_j \beta_{\perp j} (1 - \frac{\beta_{\perp j}}{\beta_{\parallel j}}) < 0$ [10]. A correction (replacing Δ_j by $2\Delta_j$) in the matrix element $M_{v_{jz}, B_{x1}}$ is required to give the same mirror instability threshold of the kinetic bi-Maxwellian plasma prediction since there is an extra factor 2 in the bi-Maxwellian expression [11], i.e.,

$$\delta p_{\perp} = 2p_{\perp} \left(1 - \frac{p_{\perp}}{p_{\parallel}} \right) \delta B_{\perp}, \quad \leftarrow \text{should be } \delta B_{\perp} / B_0 \quad (9)$$

when compared to (4). A similar difference for the mirror instability solutions of the single-fluid MHD and the bi-Maxwellian kinetic equations also exists [12].

Fig. 2 shows the thresholds of the two instabilities versus β_{\perp} for $\beta_{\parallel, \perp e} = 0$ and $\beta_{\parallel i} = 8$. The non-relativistic results for both with and without the factor 2 corrected mirror instabilities are given. For the without-correction case, the mirror instability threshold should be $1 + \sum_j \frac{\beta_{\perp j}}{2} (1 - \frac{\beta_{\perp j}}{\beta_{\parallel j}}) < 0$, which is confirmed in Fig. 2(a). We see that in general the numerical and analytical results agree. It should be pointed out that the CGL anisotropic fluid model (not considered) can involve other terms originating from the transformation of $\delta \mathbf{B}$ to δP .

3.3. Relativistic beam modes

We now test the results of Bret [3]. The ions are immobile. For the beam electrons, we have $\gamma_b = 4.0$ and $n_b = 0.1n_p$, where the

Figs.1,4,5, xlabel 'kc' should be 'kc/omega_ce', although omega_ce=1 in these test cases

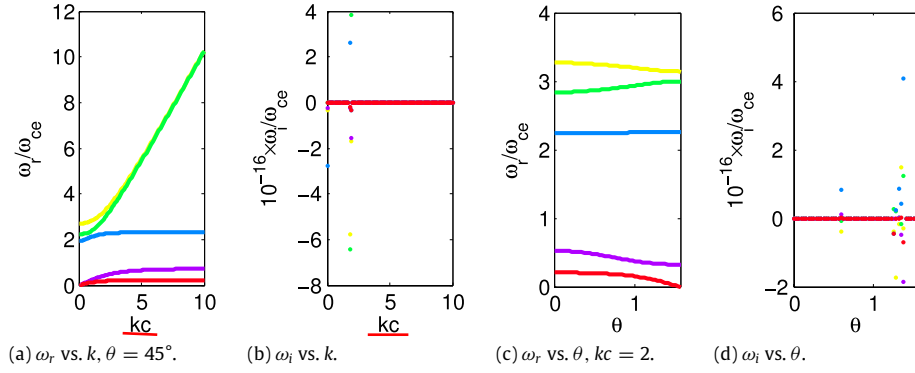


Fig. 1. The dispersion curves $\omega_{r,i}$ versus k and θ for $m_i/m_e = 4$ and $\omega_{pe} = 2\omega_{ce}$.

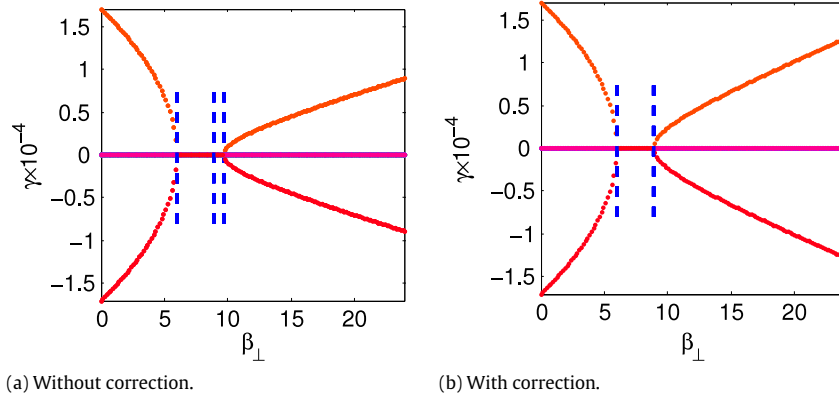


Fig. 2. The firehose and mirror instability thresholds. The dash lines are from the analytical predictions. $\beta_z = 8$, $k_z/k_\perp = 0.01$.

Table 3

Comparison of the relativistic beam plasma solutions from the PDRF and Bret's code [3].

$B_0 = 0$	ω^M	3.2736	3.2731	0.9934	0.3000	0.3000	0.2890-i0.1664	0.2890+i0.1664
	ω^B	3.2736	3.2731	0.9934	0.3000	0.3000	0.2890-i0.1664	0.2890+i0.1664
Unmagnetized	ω^M	E-16	0.0000	-0.0300	-0.0300	-1.0313	-3.2732	-3.2736
	ω^B	0	0	-0.0300	-0.0300	-1.0313	-3.2732	-3.2736
$B_0 \neq 0$	ω^M	3.2945	3.2693	1.3427	0.5168	0.0771	0.2999+i0.0034	0.2999-i0.0034
	ω^B	3.2945	3.2693	1.3427	0.5168	0.0771	0.2999+i0.0034	0.2999-i0.0034
Magnetized	ω^M	0.0440	E-16	E-16	-0.1019	-1.3983	-3.2732	-3.2910
	ω^B	0.0440	0	0	-0.1019	-1.3983	-3.2732	-3.2910

subscripts b and p denote the beam and background electron quantities, respectively. For the background electrons we have $v_p = -v_b n_b / n_p$. For $(Z_x, 0, Z_z) = \mathbf{k}v_b / \omega_{pp} = (0.3, 0, 3.0)$, the PDRF result ω^M and Bret's result ω^B are listed in Table 3. We see that they are indeed the same for both magnetized ($B_0 \neq 0$, $\omega_{ce} = \omega_{pp}$) and unmagnetized ($B_0 = 0$) plasmas.

Fig. 3 shows the maximum growth rate of the beam mode. To produce the results in Fig. 3, the Bret method using *Mathematica* takes about 1 min, whereas PDRF using *MATLAB* takes a few seconds.

3.4. The Doppler effects

In the traditional non-relativistic multi-fluid or kinetic plasma systems, the Maxwell equations are Lorentz invariant and the conservation equations are Galilean invariant, so that the overall system is neither Galilean invariant

$$\mathbf{k}' = \mathbf{k}, \quad \omega' = \omega - \mathbf{k} \cdot \mathbf{v}_0, \quad (10)$$

nor Lorentz invariant

$$\mathbf{k}' = \gamma(\mathbf{k}_\parallel - \mathbf{v}_0 \omega / c^2) + \mathbf{k}_\perp, \quad \omega' = \gamma(\omega - \mathbf{k} \cdot \mathbf{v}_0), \quad (11)$$

which can lead to inaccurate treatment of the Doppler effects. For instance, the solutions (both the frequency and the growth rate) for the electron beam system ($v_{e0} = v_d$, $v_{i0} = 0$) and the reverse ion beam system ($v_{e0} = 0$, $v_{i0} = -v_d$) would be very different, although these two systems are equivalent under a coordinate transformation. On the other hand, the relativistic multi-fluid plasma equations should be Lorentz invariant.

We now consider the Lorentz invariant (11) for the single-ion ($s = e, i$) relativistic cold plasma modes. The relativistic background density is $n_0 = \gamma(v_0)n_0^0$, where v_0 is the velocity of the moving frame. The initial parameters are $m_i = 4$, $m_e = 1$, $q_i = -q_e = 1$, $n_i = n_e = 4.0$, $v_0 = 0$, $v_{i0z} = v_0$, $v_{e0z} = 0$, $k_x c = 0.5$, and $k_z c = 1.0$, which lead to several solutions. For convenience, we consider the solution $\omega = 2.792204183976196$ (which corresponds to the largest real ω) and go to the ion moving frame with $v'_{i0z} = 0$ (but $v'_{e0z} = -v_0$), which leads to $k'_x c = 0.5$ and $k'_z c = -3.471022809144551$. The electron and ion densities then become $n'_{e0} = 9.176629354822472$ and $n'_{i0} = 1.743559577416269$, respectively. Using these new parameters, PDRF gives the largest real part solution $\omega'_M = 4.341014114998466 + 0i$, and (11) yields $\omega'_L = 4.341014114998465 + 0i$. Therefore, the difference between ω'_M and ω'_L is only in the last decimal place.

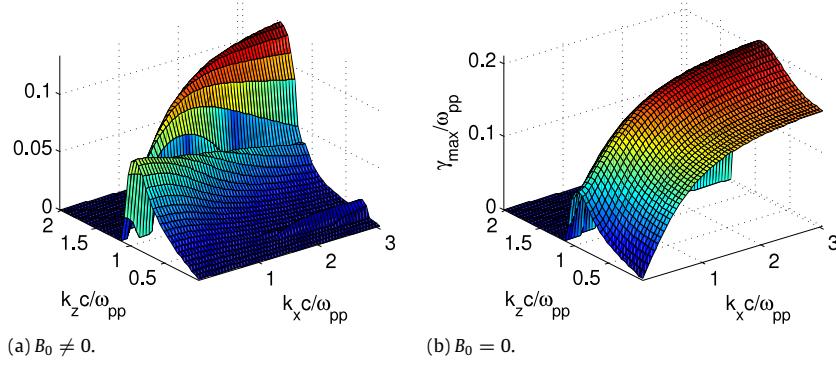


Fig. 3. The maximum growth rate γ_{\max} vs. (k_x, k_z) for the relativistic electron beam mode with and without background B_0 .

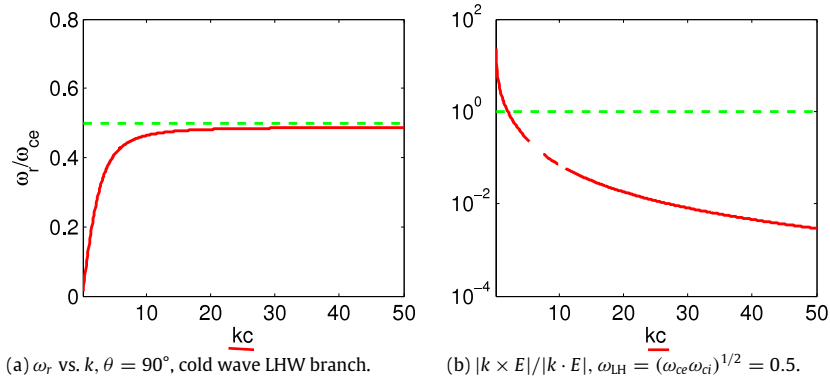


Fig. 4. Dispersion and polarization of the quasi-electrostatic cold-plasma LHW. One can see that for large kc , (a) the numerical solution $\omega_r(k)$ (red curve) approaches the analytical value $\omega_{\text{LH}} = \sqrt{\omega_{\text{ci}}\omega_{\text{ce}}}$ (green dashed line), and (b) the expression $|\mathbf{k} \times \mathbf{E}_1|/|\mathbf{k} \cdot \mathbf{E}_1|$ (red curve) for $\omega_{\text{LH}} = 0.5$ becomes very small, i.e., $\simeq 10^{-2} \ll 1$ (green dashed line).

For the $\Im\omega \neq 0$ modes, the Doppler shifted wave vector is not limited to a real number but can be complex, which is also supported by PDRF. In principle, one can also consider the effects of non-parallel beams, as well as that of v_{ij} and \mathbf{P} , on the Doppler shift.

3.5. Low hybrid wave polarization and gradient drift instability

The lower hybrid wave (LHW, $k_{\parallel} \simeq 0$) is a quasi-electrostatic mode, i.e., $|\mathbf{k} \times \mathbf{E}_1| \ll |\mathbf{k} \cdot \mathbf{E}_1|$. The polarization property of the LHW obtained from PDRF is shown in Fig. 4, which confirms the quasi-electrostatic nature of the wave.

Another interesting benchmark is the LH drift wave [13,14],

$$1 - \frac{\omega_{pi}^2}{(\omega - kv_0)^2} + \frac{\omega_{pe}^2}{\omega_{ce}^2} \left(1 + \frac{\omega_{pe}^2}{k^2 c^2} - \frac{\omega_{ce} \epsilon_n}{k\omega} \right) = 0, \quad (12)$$

where ϵ_n is the gradient parameter and $v_0 = v_{j0} - v_{e0}$ is the drift velocity in the electron frame, which can be due to the density or pressure gradient or $\mathbf{E}_0 \times \mathbf{B}_0$. The equilibrium drift velocity is $\mathbf{v}_{j0} = \mathbf{v}_{Dj} = -\frac{r_j}{q_j B_0} \nabla(\ln n_{j0}) \times \hat{\mathbf{b}}_0$.

For $v_0 = 0$ and $\epsilon_n = 0$, (12) yields the usual LHW solution, which is very close to the PDRF solution, as shown in Fig. 5(a) and (b). For $v_0 \neq 0$, a typical result is shown in Fig. 5(c) and (d), for $\epsilon_{niy} = \epsilon_{ney} = \epsilon_n = -0.15$ and $v_{i0x} = -v_{e0x} = v_0/2 = 0.01$. We can see that the PDRF solutions also qualitatively agree with (12). The quantitative disagreement can be attributed to the fact that the dispersion relation (12) is approximate and is derived using a Galilean transformation, whereas PDRF is more exact and is not Galilean invariant. For example, for cold plasmas with $v_0 = 0$ but $\epsilon_n \neq 0$, the first row of the matrix \mathbf{M} is zero, so that ϵ_n does not affect the solutions, whereas ϵ_n will affect (12) when $v_0 \neq 0$.

3.6. Other effects

In PDRF, the effects of the pressure \mathbf{P} , the density gradient $\nabla n_0/n_0$ (for local inhomogeneity) and collisions v_{ij} are given by simple models and the relativistic effects of these parameters have not been included. However, it is easy to modify the Eqs. (1) and (2), or the corresponding matrices \mathbf{A} and \mathbf{M} , when improvement of the model equations is needed.

4. Discussion

Usually one identifies a wave through its frequency. To see its other properties such as the polarization, one should also evaluate its eigenvectors. For example, strictly speaking, a pure shear Alfvén wave should not involve pressure perturbations, and a pure ion acoustic wave (IAW) should not involve magnetic perturbations. In the preceding section, we have used the eigenvector to verify the quasi-electrostatic property of LHW. The information of the eigenvectors can be useful for identifying different waves having the same or nearly the same frequencies, for efficiently exciting specific waves by fixing the initial condition or the source (such as an antenna), for diagnostics of more detailed properties of the waves, etc. This is because the perturbations in a system are given by $X = \sum_j c_j X_j$, where X_j are the eigenvectors of the eigenmode and c_j is the corresponding coefficient. The power spectrum of a single wave parameter (e.g., n_1 or B_{x1}) cannot accurately determine the coefficients, since different parameter values will give different power spectrums.

With conventional dispersion relation solvers, usually only the wave frequency is obtained. One has to obtain the corresponding eigenvectors separately. PDRF provides a way to obtain the eigenvectors together with the eigenvalues.

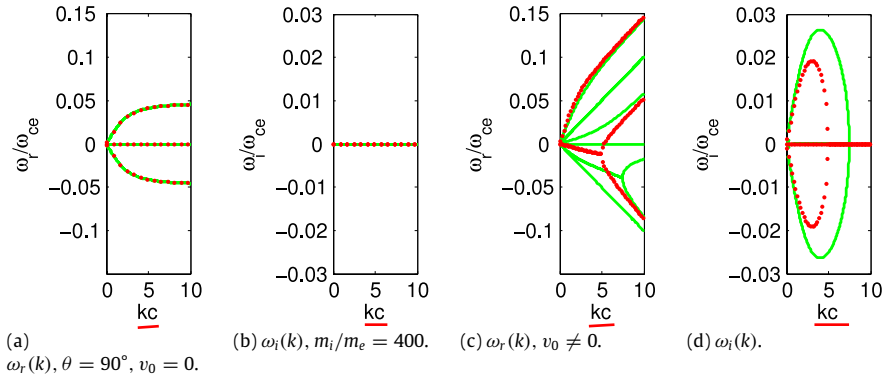


Fig. 5. Low hybrid drift instability. Red dot lines are solutions from (12) with transformation $\omega' = \omega - kv_0/2$.

To summarize, in this paper a general multi-fluid dispersion relation solver is provided, which shows good performance in several benchmark cases. The solver can include effects that cannot be handled by conventional solvers. The full-matrix treatment provides a general and accurate method for obtaining the dispersion relation of waves in complex fluid plasma systems. A similar treatment for kinetic plasma systems is still under development.

Acknowledgments

The author would like to thank M.Y. Yu for improving the manuscript. This work is partly inspired when the author was collaborating with Liu Chen, W. Kong, Y. Lin and X.Y. Wang in the GeFi project. Discussions and comments from Y. Xiao and Ling Chen are also appreciated. This work is supported by Fundamental Research Fund for Chinese Central Universities.

Appendix A. Extension to unmagnetized plasmas

Setting $\mathbf{B}_0 = 0$ in PDRF, we can obtain a simple unmagnetized-plasma version solver, such as shown in Fig. 3. For an unmagnetized plasma, we need a new treatment for the anisotropic pressure, since there is no parallel background \mathbf{B}_0 . Here, for the pressure $P_{\parallel j}$ and $P_{\perp j}$, the \parallel and \perp are parallel and perpendicular to \mathbf{v}_j when $\mathbf{v}_{j0} \neq 0$. Without loss of generality, we set $\mathbf{k} = (0, 0, k_z)$.

A rotation matrix

$$\mathbf{R}_j = \mathbf{R}_{jy} \cdot \mathbf{R}_{jx} = \begin{bmatrix} \cos \phi_j & 0 & \sin \phi_j \\ 0 & 1 & 0 \\ -\sin \phi_j & 0 & \cos \phi_j \end{bmatrix} \cdot \begin{bmatrix} 1 & 0 & 0 \\ 0 & \cos \theta_j & -\sin \theta_j \\ 0 & \sin \theta_j & \cos \theta_j \end{bmatrix} = \begin{bmatrix} \sqrt{v_{jy}^2 + v_{jz}^2} & -v_{jx}v_{jy} & -v_{jx}v_{jz} \\ v_j & v_j\sqrt{v_{jy}^2 + v_{jz}^2} & v_j\sqrt{v_{jy}^2 + v_{jz}^2} \\ 0 & v_{jz} & -v_{jy} \\ \frac{v_{jx}}{v_j} & \frac{v_{jy}}{v_j} & \frac{v_{jz}}{v_j} \end{bmatrix}, \quad (\text{A.1})$$

is required to transform $\hat{\perp}_j$ and $\hat{\parallel}_j$ to \hat{x} , \hat{y} , \hat{z} , i.e., the pressure tensor should be

$$\mathbf{P}_j = \mathbf{R}_j^T \cdot \begin{bmatrix} P_{\perp j} & 0 & 0 \\ 0 & P_{\perp j} & 0 \\ 0 & 0 & P_{\parallel j} \end{bmatrix} \cdot \mathbf{R}_j, \quad (\text{A.2})$$

which yields

$$\begin{aligned} P_{jxx} &= P_{\perp j} + (P_{\parallel j} - P_{\perp j}) \frac{v_{jx}^2}{v_j^2}, & P_{jyy} &= P_{\perp j} + (P_{\parallel j} - P_{\perp j}) \frac{v_{jy}^2}{v_j^2}, \\ P_{jzz} &= P_{\perp j} + (P_{\parallel j} - P_{\perp j}) \frac{v_{jz}^2}{v_j^2}, \\ P_{jxy} &= P_{jyx} = (P_{\parallel j} - P_{\perp j}) \frac{v_{jx}v_{jy}}{v_j^2}, \\ P_{jzx} &= P_{jxz} = (P_{\parallel j} - P_{\perp j}) \frac{v_{jx}v_{jz}}{v_j^2}, \\ P_{jzy} &= P_{jyz} = (P_{\parallel j} - P_{\perp j}) \frac{v_{jy}v_{jz}}{v_j^2}. \end{aligned} \quad (\text{A.3})$$

For $\mathbf{v}_{j0} = 0$, one should set $\mathbf{P}_j = P_j$ as a scalar quantity.

Treatment for other unmagnetized plasmas are similar to that for the magnetized plasma. The above description provides a guide for developing a more general unmagnetized plasma version of PDRF.

Appendix B. PDRF user manual

PDRF consists of two files: the main program “pdrf.m” and the input data file “pdrf.in”. The input file has the following structure:

```
qs      ms      ns      vsx      vsy      vsz      csz      csp      epsnjx  epsnjl
-1.0    1.0    4.0    0.0     0.0     0.0     0.0     0.0     0.0     0.0
1.0     4.0    4.0    0.0     0.0     0.0     0.0     0.0     0.0     0.0
```

One can add the corresponding parameters for additional species.

Normalizations and other parameters can be reset in “pdrf.m”. Since PDRF is a short code, one can also easily modify the default setup for other applications.

References

- [1] K. Ronnmark, KGI Report No. 179, Sweden, 1982.
- [2] K. Ronnmark, Plasma Phys. 25 (1983) 699.
- [3] A. Bret, Comput. Phys. Comm. 176 (2007) 362.
- [4] T. Stix, Waves in Plasmas, AIP Press, 1992.
- [5] A. Bret, C. Deutsch, Phys. Plasmas 13 (2006) 042106.
- [6] G.F. Chew, M.L. Goldberger, F.E. Low, Proc. R. Soc. A236 (1956) 112.
- [7] J. Goedbloed, S. Poedts, Principles of Magnetohydrodynamics: With Applications to Laboratory and Astrophysical Plasmas, Cambridge, 2004.
- [8] A. Hakim, J. Fusion Energy 27 (2008) 36.
- [9] D.G. Swanson, Plasma Waves, second ed., IOP, 2003.
- [10] A. Hasegawa, Plasma Instabilities and Nonlinear Effects, Springer, 1975.
- [11] D.J. Southwood, M.G. Kivelson, J. Geophys. Res. 98 (1993) 9181.
- [12] L.N. Hau, B.U. Sonnerup, Geophys. Res. Lett. 20 (1993) 1763.
- [13] N.A. Krall, P.C. Liewer, Phys. Rev. A 4 (1971) 2094.
- [14] K. Yatsui, T. Imai, M. Furumi, J. Phys. Soc. Japan 42 (1977) 652.